Malaysian Journal of Chemistry, 2021, Vol. 23(1), 33-47

The Anticancer Activity of Oleanane-type Saponin from *Bombax ceiba (in vitro)* and Theoretical Investigation of Signaling Pathway

Mohd Rehan and Shafiullah*
Department of Chemistry, Aligarh Muslim University, Aligarh-202002, Uttar Pradesh, India
*Corresponding author (e-mail: shafiullah1966@gmail.com)

Bombax ceiba is a traditional medicinal tree that is useful in the treatment of anti-tumor, anti-microbial, anti-oxidant, colds, coughs, etc. *β*-amyrin is a biologically active compound that was isolated from the EtOH extract of *B. ceiba* leaves. This work describes the anticancer activity of the leaf extract and isolated compound against human breast (MDA-MB-231 and BT-549), lung (A-549) and colon (SW-480) cancer cell lines, and the relation of the compound with anticancer activity was supported by molecular docking. The structure of the isolated compound was confirmed by the methods of ^{1}D-NMR, ^{2}D-NMR, and mass spectrometry data. The anticancer activity of the EtOH leaf extract and isolated compound was determined on colon, breast, and lung cancer cell lines by MTT assay. Docking studies of the isolated compound were done with the help of softwares such as Discovery Studio Visualizer, chem3D pro 12.0.2.1076, Auto Dock Tools-1.5.6, and Auto dock vina. The structure of the isolated compound was confirmed as 3β-olean-12-en-3-ol (*β*-amyrin). *β*-amyrin and the EtOH leaf extract both showed high inhibitory activities on BT-549 cancer cell line. The docking studies of the isolated compound exhibited best docking scores with PI3K and mTOR. From the best docking scores, it was clear that *β*-amyrin has a high probability of target of PI3Kα and mTOR. The anticancer activity of the EtOH leaf extract of *Bombax ceiba* and its isolated *β*-amyrin showed excellent anticancer activities on breast cancer cell lines and *β*-amyrin showed high inhibitory activities with PI3Kα and mTOR kinases by docking studies.

Key words: *Bombax ceiba*; COSY; MDA-MB-231; BT-549; PI3Kα; mTOR

Received: June 2020; Accepted: October 2020

Bombax ceiba (red silk-cotton tree) is a member of the family Bombaceae which is cultivated in India, Pakistan, Sri Lanka, Malaysia, Bangladesh, and North Australia. This tree is widely planted in southeastern Asian countries, such as southern China, Indonesia, Vietnam, Malaysia, Thailand, Taiwan, Myanmar, etc. It is found in the book 'The Useful Native Plants of Australia' (1889) that *B. ceiba* was known at that time as *Bombax malabaricum*, and the common name was Malabar silk-cotton of India, or Simool [1]. It is known as cotton-tree flowers in China, which plays an important role in Cantonese culture in Southern China.

This tree has been used in health care since ancient times worldwide. The history of this plant as medicines is very long because parts of this plant have been used in traditional system of medicine, such as Unani, Siddha, Ayurveda, and Traditional Tibetan and Chinese medicine [2-3]. In traditional Unani medicine (better known as Hippocrates, 460-377 BC), parts of this plant are used in tonic, aphrodisiac, astringent, demulcent, and to increase semen production and count [4]. A traditional Chinese formulation containing *B. ceiba* is used in eliminating food retention in the intestines, promotes digestion, and strengthens the spleen [5]. This plant is used in formulation of Ayurveda for anti-dysenteric effects, wound healing, and tissue regeneration [6]. This plant has high importance which have been utilized since the Han dynasty (second century BC). The seed powder of *B. ceiba* with hing and sugar molasses given in 12 h gap to induce abortion by the *Oraon* tribe [7].

According to T. P. Ghose, chemical studies of this plant were first started on the roots in 1935. Then, several compounds were isolated from many parts [8]. Previous phytochemical studies highlighted the presence of flavonoids, quinines, sterols, saponins, fatty acids, and hydrocarbons [9], as well as various promising activities such as anti-tumour, anti-microbials [10], anti-oxidant, cytotoxicity [11], and anti-proliferative [12]. *β*-Amyrin is a known compound which has been isolated from many plants, such as *Bombax ceiba* [13], *Himatanthus drasticus* [14], *Protium paniculatum* [15], and *Myrcianthes pungens* [16]. This compound has been used for many pharmacological activities, such as anti-diabetic, anti-hyperlipidemic, anti-nociceptive, anti-inflammatory [17-20], apoptosis [21], Alzheimer's [22], and anti-hyperglycemic [23].

Previous studies reported that extracts of this plant had been used on human cancer cell lines such as

HL60, LNCap, MCF-7, HeLa, A-375, and THP-1 [24-25], and an isolated compound had been used in anti-tumor effects on liver carcinoma cell line (HepG2) [26]. The cytotoxic activity of *β*-amyrin had also been evaluated on colorectal carcinoma (Caco-2) [27]. This compound was used for cell growth inhibition on SK-OV-3 (ovary), HeLa (cervical), DLD-1 (colon), and SW-620 (colon) cancer cell lines [28]. This compound also exhibited potent anti-tumor activity against HK-1 (human nasopharyngeal cancer cell line) [29]. Our report describes the EtOH leaf extract and *β*-amyrin analyzed for anti-cancer activities against MDA-MB-231, BT-549, SW-480, and A-549 human cancer cell lines (*in vitro*), and docking studies of *β*-amyrin performed with various proteins (*in silico*).

β-amyrin was studied against proteins such as P^{53}, AKT, BCl_2, IGFR, mTOR, PTEN, KRAS, PI3Kα, PI3Kβ, etc. Best molecular docking results were obtained from PI3K and mTOR. Therefore, this compound is useful for the target of the PI3K/AKT/mTOR signaling pathway. This pathway plays important roles in survival, development, proliferation, differentiation, and metabolism. It has been found in various studies that the PI3K/AKT/mTOR pathway is present in all human tumors, including breast cancer. More than 60% of tumors of different variations are presented with hyperactivation of this pathway [30]. Disregulation of this pathway relates to different types of cancer, including metabolic reprogramming, genomic instability, and uncontrolled proliferation in tumor cells [31-32]. Activation of the PI3K/AKT/mTOR pathway is the main cause of resistance of cancer cells to chemotheraties [33]. Study of the PI3K/AKT/mTOR pathway plays an important role in understanding the progression and development of this disease [34-35].

MATERIALS AND METHODS

General Experimental Procedures

Thin layer chromatography analysis glass plates (200 × 200 × 3 mm and 200 × 50 × 3 mm) were coated with silica gel GF_{254} (Sisco Research Laboratories and Alfa Aesar) and spots of the compound were visualized under iodine chamber (270 × 265 × 70 mm) and UV light (254 nm and 366 nm). Column chromatography was performed in a silica gel open glass column (60 inch × 35 mm), using silica gel (60-120 mesh, Merck, India). Measurement of the melting point was done on Stuart digital melting point apparatus (SMP10). The structural assignment of the compound was based on IR (infrared), ^{1}H-NMR, ^{13}C-NMR, DEPT, HSQC, and COSY spectra. IR spectra were determined on Perkin-Elmer Spectrum 2 (FTIR) instrument (Perkin Elmer, Singapore), using KBr discs. The NMR spectral analysis was acquired in $CDCl_3$, as solvent, on Bruker Avance II NMR spectrometer (Bruker BioSpin, Fallanden, Switzerland) at 400 MHz (^{1}H-NMR) and 100 MHz (^{13}C-NMR), and chemical shifts were reported in parts per million (δ). The chemical shifts of the solvent peaks were used for referencing ($CDCl_3$; δ_H 7.26 and δ_C 77.16) and coupling constant (J) were reported in hertz (Hz). The isolated compound was dissolved in 0.75 ml of $CDCl_3$ with 0.03% TMS as an internal standard. Distortionless Enhancement by Polarization Transfer (DEPT) and ^{2}D-NMR [^{1}H-^{1}H COSY (Correlation Spectroscopy), HSQC (Heteronuclear Single Quantum Correlation)] were acquired on Bruker Avance II NMR spectrometer (Bruker BioSpin, Fallanden, Switzerland). ^{1}D (^{1}H-NMR and ^{13}C-NMR) and ^{2}D-NMR were performed at 30^O with standard pulse program and the spectra were processed using MestReNova-11.0 software. HR-MS chromatogram was acquired on a high resolution mass spectrometer XEVO G2-XS QTOF instrument (Water India Pvt. Ltd., Bangalore, India). Solvents, such as petroleum ether ($60–80^OC$), benzene, ethyl acetate, ethanol, chloroform, dimethylsulfoxide (DMSO) were purchased from E-Merck, India. Fetal bovine serum (FBS) was obtained from GIBCO Invitrogen Corporation, USA. RPMI-1640 medium, penicillin, streptomycin, and 3-(4,5,-dimethylthiazole-2-yl)-2,5-diphenyltetrazolium bromide (MTT) were purchased from Sigma –Aldrich (Bangalore, India).

Extraction and Isolation

The shade air-dried plant leaf material (2 kg) was extracted with 82% EtOH (ethanol) at 25^OC for 15 days. The crude extract was filtered and collected using a Buchner funnel and concentrated under reduced pressure to yield 110 g of solid residue. The EtOH residue (110 g) was partitioned using stepwise solvent C_6H_6 and EtOAc (ethyl acetate) to yield benzene extract (28 g) and ethyl acetate extract (35 g). The C_6H_6 extract was fractionated by silica gel (60-120 mesh) column chromatography, eluted with a step gradient petroleum-ether: C_6H_6/petroleum-ether: benzene (100:0/0:100 v/v) as the mobile phase at the flow rate of 6 ml/min to give seven main fractions, P1-P7. Each fraction was collected and monitored based on the TLC (GF_{254}) analysis. Fraction P5 was further separated on silica gel by column chromatography with the stepwise gradient from petroleum-ether/C_6H_6 (50/50 v/v) to pure C_6H_6 as the mobile phase at the flow rate of 6 ml/min to yield five subfractions ($P5_1$-$P5_5$). Subfraction $P5_3$ was further purified by silica gel glass chromatography using gradient petroleum-ether/C_6H_6 (30/70 v/v) to give one compound (145 mg). Compound $P5_3$ was recrystallised in 5 ml of pure chloroform at room temperature. After two days, the compound was precipitated out in a 25 ml conical flask. The precipitate was filtered using a Buchner funnel under reduced pressure and washed with 2 ml of pure chloroform. After filtration, we obtained a white solid, which was dried at room temperature. After recrystallization, the compound was further analyzed by melting point and IR, ^{1}D-NMR, ^{2}D-NMR, and HR-MS spectral techniques (summarized in Table 1).

Cell Culture, Growth Conditions and Treatment

Human breast cancer cell lines (MDA-MB-231 and BT-549), colon cancer cell line (A-549) and lung cell line (SW-480) were procured from the National Cancer Institute (NCI), Bethesda, USA. The cancer cell lines were cultured in RPMI-1640/minimum essential medium (MEM) supplemented with 10% fetal bovine serum (FBS), 100 U/ml of penicillin and 100 µg per ml of streptomycin at 37^{O}C in 5% CO_2 gas environment and 95% air atmosphere with 98% humidity. The cell lines were treated with the EtOH leaf extract and *β*-Amyrin dissolved in dimethylsulfoxide (DMSO), while the untreated cultures received only the vehicle (DMSO, <0.2%, v/v).

Cell Viability Assay by MTT

The effects of the leaf extract and the compound on the viability of MDA-MB-231, SW480, A549, and BT549 were determined by MTT assay. All the human cancer cell lines were seeded in 96- well culture plates at a density of 1 × 10^4/200 µl of the medium. Cells were treated with the extract and compound at different concentrations for 48 hours. MTT was added and incubated at 37°C in a CO_2 incubator (Thermocon Electron Corporation, USA) for 4 hours. Formazan blue crystals were formed by viable cells that were dissolved in 200 µl of DMSO, and finally the absorbance was measured at a wavelength of 570 nm (reference wavelength of 620 nm) with ELISA reader. The percentages of cell viability was calculated according to the following equations [36].

Cell viability (%) = $[(OD_{\text{treated cells}} - OD_{\text{blank}})/ (OD_{\text{control}} - OD_{\text{blank}})] \times 100\%$

OD = Optical Density

Molecular Docking Studies

The 3D crystal structures of kinases of [PI3K*α* (PDB ID: 4L23) and mTOR (PDB ID: 4JT6)] were retrieved from the RCSB protein data bank. The ligands and water molecules were removed to stabilize the kinase structures by BIOVIA Discovery Studio 2017 R2 software. The kinases were prepared for the docking process, then loaded to Auto Dock Tools-1.5.6 software to identify the binding sites of PI3Kα and mTOR and assign polar hydrogen and kollman charges to minimize proteins. Grids were generated for the binding site in the active centers and compound-bound interaction points. A grid box was set with a dimension of 126 × 126 × 94 (X × Y × Z), grid spacing 1A^{O} and center X = Y = Z = 0.028 for PI3Kα. A grid box was set with a dimension of 126 × 126 × 126 (X × Y × Z), grid spacing 1A^{O} and center X = Y = Z = 0.028 for mTOR. The 3D crystal structure of the compound was done by using Chem3D Pro 12.0.2.1076 and saved as a Protein Data Bank (PDB) file. The compound was loaded to Auto Dock Tools to re-assign kollman charges and hydrogen atoms. All rotatable bonds (torsions) were auto-detected and gave different poses in molecular docking. Finally, molecular docking of β-amyrin with kinases was performed by Autodock Vina software.

RESULTS

Spectroscopic Data of 3β-olean-12-en-3-ol

The compound was isolated as a white amorphous solid; m.p.: 206^{O}C; IR (KBr, cm^{-1}): 3292 (OH), 2946 and 2869 (CH), 1633 (C=C), 1463 (CH_2); ^{1}H-NMR (400 MH_Z, $CDCl_3$, *δ* / ppm): 5.19 (1H, *t*, *J* = 3.52 Hz, H-12), 3.24 (1H, *dd*, *J*= 4.6 Hz, 11.4 Hz, H-3), 1.98 (*m*, H-15), 1.87 (*m*, H-11), 1.76 (*m*, H-16), 1.69 (*m*, H-19), 1.61 (*m*, H-1), 1.60 (*m*, H-2), 1.54 (*m*, H-6), 1.51 (*m*, H-7), 1.41 (*m*, H-22), 1.38 (*m*, H-21), 1.13 (3H, *s*, H-27), 0.99 (3H, *s*, H-24), 0.96 (3H, *s*, H-26), 0.93 (3H, *s*, H-25), 0.87 (6H, *s*, H-29, 30), 0.83 (3H, *s*, H-28), 0.78 (3H, *s*, H-23), 1.54 (1H, *m*, H-9), 1.54 (1H, *m*, H-18), 0.71 (1H, *dd*, *J* = 2.3 Hz, 10.8 Hz, H-5); ^{13}C-NMR (100 MHz, $CDCl_3$, *δ* / ppm): 145.16 (C-13), 121.69 (C-12), 78.98 (C-3), 55.14 (C-5), 47.70 (C-9), 47.44 (C-18), 46.89 (C-19), 41.67 (C-14), 39.76 (C-8), 38.75 (C-4), 38.55 (C-1),37.11 (C-22), 37.07 (C-20), 36.91 (C-10), 34.70 (C-21), 33.35 (C-29), 32.61 (C-7), 32.61 (C-17), 28.37 (C-28), 15.43 (C-23), 27.19 (C-2), 26.90 (C-15), 26.12 (C-16), 25.9 (C-27), 23.65 (C-30), 23.51 (C-11), 18.39 (C-6), 16.76 (C-26), 15.54 (C-25), 28.0 (C-24); HSQC ($CDCl_3$, *δ* / ppm): C-1 (38.55, 1.61, 1.02; CH_2), C-2 (27.19, 1.60, 0.80; CH_2), C-3 (78.98, 3.24; CH), C-5 (55.14, 0.71; CH), C-6 (18.39, 1.54, 1.41; CH_2), C-7 (32.61, 1.51, 1.35; CH_2), C-9 (47.70, 1.54; CH), C-11 (23.51, 1.87; CH_2), C-12 (121.69, 5.19; CH), C-15 (26.90, 1.98; CH_2), C-16 (26.12, 1.76, 0.95; CH_2), C-18 (47.44, 1.54; CH), C-19 (46.89, 1.69, 1.07; CH_2), C-21 (34.70, 1.38, 1.18; CH_2), C-22 (37.11, 1.41, 1.23; CH_2), C-23 (15.43, 0.78; CH_3), C-24 (28.0, 0.99; CH_3), C-25 (15.54, 0.93; CH_3), C-26 (16.76, 0.96; CH_3), C-27 (25.9, 1.13; CH_3), C-28 (28.37, 0.83; CH_3), C-29 (33.35, 0.87; CH_3), C-30 (23.65, 0.87; CH_3); HR-MS (*m/z*): 427.3933 $(MH)^+$.

Table 1. ^{1}H-NMR, ^{13}C-NMR, DEPT and COSY spectroscopic data of isolated compound[a]

Atom	Type	δ_C	δ_H	^{1}H-^{1}H COSY
1	CH_2	38.55	1.61 (Ha_1), 1.02 (Hb_1)	Hb_2
2	CH_2	27.19	1.60 (Ha_2), 0.80 (Hb_2)	Hb_1, H-3
3	CH	78.98	3.24 (*dd*) [*J* = 4.6, 11.4]	Ha_2
4	C	38.75	------	------
5	CH	55.14	0.71 (*dd*) [*J* = 2.3, 10.8]	Hb_6
6	CH_2	18.39	1.54 (Ha_6), 1.41 (Hb_6)	H-5, Ha_7
7	CH_2	32.61	1.51 (Ha_7), 1.35 (Hb_7)	Hb_6
8	C	39.76	------	------
9	CH	47.70	1.54 (*m*)	H-11
10	C	36.91	------	------
11	CH_2	23.51	1.87	H-9, H-12
12	CH	121.69	5.19 (*t*) [*J* = 3.52]	H-11
13	C	145.16	------	------
14	C	41.67	------	------
15	CH_2	26.90	1.98	Hb_{16}
16	CH_2	26.12	1.76 (Ha_{16}), 0.95 (Hb_{16})	H-15
17	C	32.61	------	------
18	CH	47.44	1.54 (m)	------
19	CH_2	46.89	1.69 (Ha_{19}), 1.07 (Hb_{19})	------
20	C	37.07	------	------
21	CH_2	34.70	1.38 (Ha_{21}), 1.18 (Hb_{21})	Ha_{22}
22	CH_2	37.11	1.41 (Ha_{22}), 1.23 (Hb_{22})	Hb_{21}
23	CH_3	15.43	0.78 (*s*)	
24	CH_3	28.0	0.99 (*s*)	
25	CH_3	15.54	0.93 (*s*)	
26	CH_3	16.76	0.96 (*s*)	
27	CH_3	25.9	1.13 (*s*)	
28	CH_3	28.37	0.83 (*s*)	
29	CH_3	33.35	0.87 (*s*)	
30	CH_3	23.65	0.87 (*s*)	

[a] All spectra run in $CDCl_3$.

Chemistry

A white amorphous powder of the compound was obtained, with melting point 206 ^{O}C. The HR-MS (High Resolution Mass Spectrometry) data revealed a protonated molecular ion peak at m/z 427.3933 $[M+H]^+$, suggesting the molecular formula of $C_{30}H_{50}O$. The infrared (IR) spectra showed absorption peaks at 3292 cm^{-1} [–OH (hydroxyl group) stretching vibration], 2946 and 2869 cm^{-1} (C-H stretching vibration), 1633 cm^{-1} (C=C stretching vibration), and 1463 cm^{-1} (CH_2 bending vibration). The ^{1}H and ^{13}C-NMR data (Table 1) showed doublet-doublet at δ_H 3.24 (*J*=4.6, 11.4) and ^{13}C-NMR at δ_C 78.98 which indicated the presence of CH at C-3 [37-38]. ^{1}H signal at δ_H 5.19 (t, *J*=3.52) and ^{13}C signals at δ_C 121.69 and δ_C 145.16 revealed the presence of one double bond. The ^{13}C-NMR and DEPT-135 (Distortionless Enhancement by Polarization Transfer) spectra resolved eight methyl carbons (δ_C: 28.0, 15.43, 15.54, 16.76, 25.9, 28.37, 33.35, 23.65), ten methylene carbons (δ_C: 38.55, 27.19, 18.39, 32.61, 23.51, 26.9, 26.12, 37.11, 34.70, 46.89), four methine carbons (δ_C: 78.98, 55.14, 47.7, 47.44). HSQC (Heteronuclear Single Quantum Coherence) spectroacopy provides correlations between carbon and its attached protons. This spectroscopy has been used in characterization of many natural products [39-40]. The HSQC spectrum showed the correlation between δ_C 38.55 (C-1) and δ_H 1.61, 1.02. ^{1}H-^{1}H COSY (Correlation Spectroscopy) displayed correlation between δ_H 1.02 and δ_H 0.80, as well as δ_H 1.60 and δ_H 3.12 (Figure 1(A)). Correlation between δ_H 1.87 and δ_H 5.1 (alkene proton) and δ_H 1.54 in ^{1}H-^{1}H COSY indicated connectivity of alkene protons. Alkene protons showed correlation from methine carbon δ_C 121.69 (C-12) in HSQC, which revealed connectivity between alkene protons and methine carbons. It was confirmed by spectroscopic methods that the isolated compound was 3β-olean-12-en-3-ol (β-amyrin). Peak assignments of β-amyrin are showed in Figure 1(B).

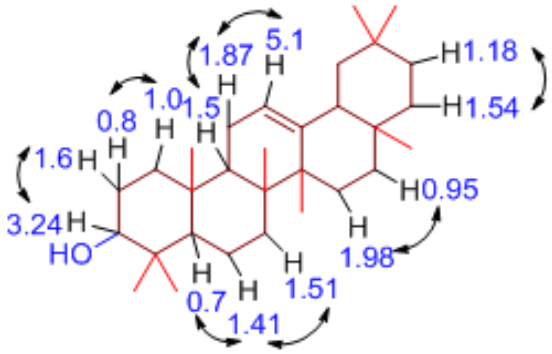

(**A**)

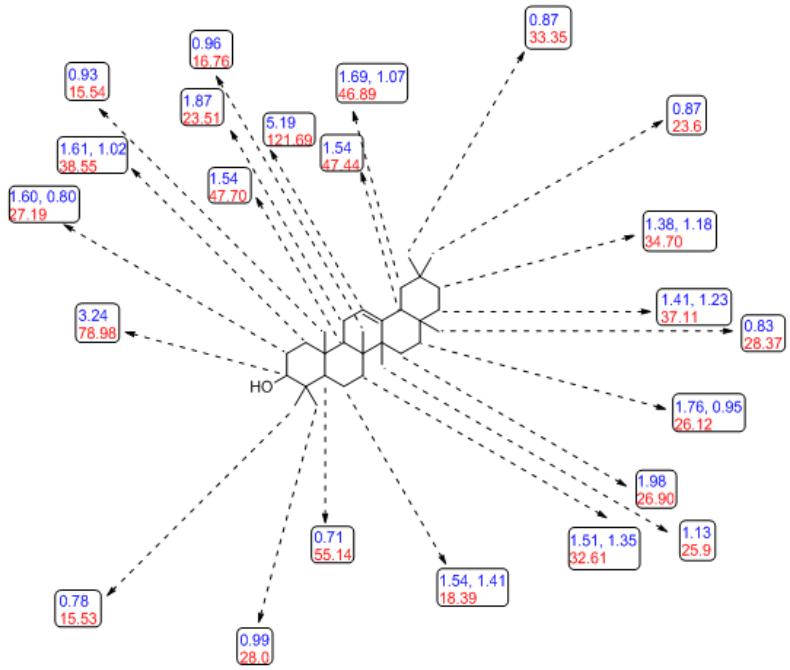

(**B**)

Figure 1. (A) COSY correlation and (B) ^{1}H-NMR, ^{13}C-NMR, DEPT-135, and HSQC peak assignments of β-amyrin

Anticancer Activities of the EtOH Leaf Extract

In vitro, anticancer activities of the leaf extract were assessed via the MTT assay on a colon cancer cell line (A-549), a lung cancer cell line (SW-480), and breast cancer cell lines (MDA-MB-231 and BT-549) for 48 hours. Figure 2(A) reveals the cell viability of all four cancer cell lines. After 48 h treatment, reduction was observed in cell viability in all cancer cell lines. The extract possessed an excellent anticancer activity against breast cancer cell line BT-549. When exposed to the EtOH leaf extract at the concentration of 100 µg/ml, the percentage of cell viability reached 54%.

Anticancer Activities of *β*-amyrin

The anticancer activities of *β*-amyrin in this work were evaluated against A-549, SW-480, MDA-MB-231, and BT-549 human cancer cell lines. The percentage of cell viability of the four cancer cell lines is presented in Figure 2(B). After 48 h treatment, reduction was observed in cell viability on all the cancer cell lines. The extract possessed an excellent anticancer activity against breast cancer cell lines BT-549 and MDA-MB-231. When exposed to *β*-amyrin at the concentration of 100 µg/ml, the percentage of cell viability reached 58% and 57% in MDA-MB-231 and BT-549, respectively.

The EtOH leaf extract and *β*-amyrin both displayed high anticancer activities against BT-549. The

extract exhibited better anticancer activities compared to *β*-amyrin.

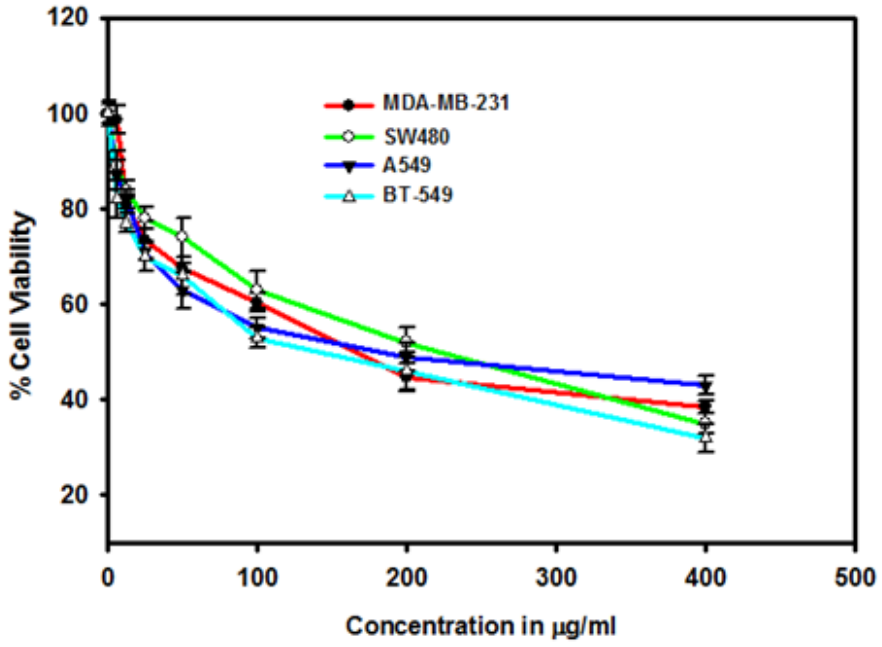

(A)

Figure 2A. Effects of the EtOH leaf extract on cell viability of MDA-MB-231, SW-480, A-549, and BT-549 cell lines. The cell lines were exposed to different concentrations (5, 10, 25, 50, 100, 200, and 400 µg/ml) of the leaf extract for 48 h and cell viability was determined by the MTT assay. At 100 µg/ml concentration of the leaf extract, viability of BT-549 was 54%.

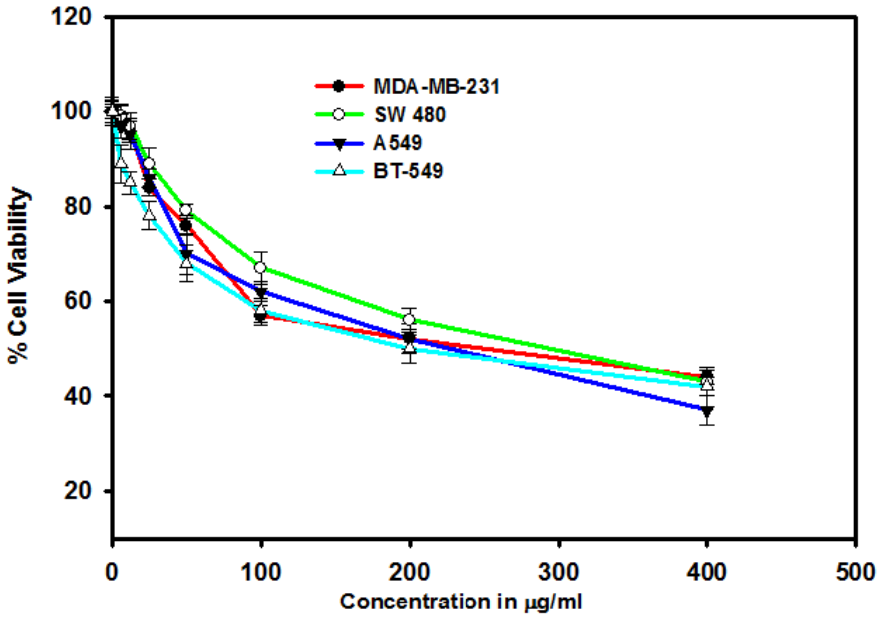

(B)

Figure 2B. Effects of *β*-amyrin on cell viability of MDA-MB-231, SW-480, A-549, and BT-549 cell lines. The cell lines were exposed to different concentrations (5, 10, 25, 50, 100, 200, and 400 µg/ml) of *β*-amyrin for 48 h and cell viability was determined by the MTT assay. At 100 µg/ml concentration of *β*-amyrin, viability of MDA-MB-231 and BT-549 was 58% and 57%, respectively.

Table 2. *In silico* optimization of *β*-amyrin

Entry	Protein	PDB	Docking score (kcal/mole)
1	P^{53}	4HJE	-8.9
2	AKT	3MV5	-8.4
3	BCl_2	4IEH	-7.9
4	EGFR	2JIT	-7.6
5	IGFR	1IGR	-6.8
6	PDK	2R7B	0.0
7	Tankyrase	5JU5	-8.8
8	**mTOR**	**4JT6**	**-9.7**
9	PTEN	1D5R	0.0
10	KRAS	6N2J	-7.6
11	**PI3Kα**	**4L23**	**-10.6**
12	PI3Kβ	2Y3A	-8.9
13	PI3Kγ	3DBS	-8.0
14	PI3Kδ	2WXG	-8.8

Molecular Docking Studies

Molecular docking studies play a key role in drug design. Various evidence indicates that PI3K/AKT/mTOR [41], PDK/AKT [42], PI3K/PTEN [43], EGFR/PI3K/PTEN/AKT/mTOR [44], IGFR PI3K [45], PI3K/PDK/AKT [46], and cJUN NH_2-terminal kinase (JNK) signaling pathways [47], and mitogen-activated protein kinases (MAPK) pathway [48] are present in breast cancer signaling pathways and play important roles in cell apoptosis, proliferation, and autophagy. Docking of *β*-amyrin was optimized for the best inhibitory target on various proteins (P^{53}, AKT, IGFR, EGFR, KRAS, PI3K, mTOR etc.) and some results are summarized in Table 2. Optimization of *β*-amyrin was done using Autodock Vina software. PI3Kα (Table 2, entry 11) exhibited an excellent docking score (-10.6 kcal/mol) with strong binding interaction, and mTOR (Table 2, entry 8) was close to PI3Kα. PI3Kα was further optimized with PI3Kβ, PI3Kγ, and PI3Kδ. PI3Kα was best in all isoforms and measured in kcal/mol. Finally, we found the best results of *β*-amyrin with PI3K and mTOR (Table 2, entries 8, 11) when screening this compound with various types of proteins which are present in many cancer signaling pathways. Various natural products, which are isolated from different plant species, have high potential in inhibition of PI3K and mTOR kinases [49–52]. The PI3K/mTOR dual inhibitor compound is best for cancer therapies.

Molecular Docking Analysis with PI3Kα isoform

The results of the docking study of *β*-amyrin with PI3Kα are presented in Figure 3. *β*-amyrin was successfully docked with PI3Kα isoform. Docking studies of *β*-amyrin with PI3Kα showed favorable binding with a docking score of -10.6 kcal/mol. The hydrogen binding and hydrophobic interaction of the compound with residues LYS, SER, TRP, VAL, and PRO were displayed on the active site of PI3Kα. The classical hydrogen binding interaction of the hydroxyl group with amino acid SER-474 at 1.98 was exhibited. The compound interacted with PI3Kα by formation of alkyl hydrophobic and mixed pi/alkyl hydrophobic bonds with the amino acids, such as: LYS-678 at 3.96, 4.12 distance with C-24 and C-25; TRP-446 at 5.37 distance with C-25; PRO-449 at 3.87, 5.13 distance with C-28; VAL-461 at 4.54 distance with C-29; and TRP-424 at 4.73 distance with C-30.

Docking Analysis with mTOR

Docking results of *β*-amyrin with mTOR can be visualized in Figure 4. *β*-amyrin with mTOR was screened and revealed the best binding with docking score of -9.7 kcal/mol. The hydrophobic binding interaction of the compound with amino acid residues such as LYS, LEU, PRO, and TRP was exhibited on the active site of mTOR. The compound was investigated with residues which displayed alkyl hydrophobic and mixed pi/alkyl hydrophobic interactions of: PRO-1646 at 3.97 distance with C-24; TRP-1653 at 4.18, 4.96, 5.04, 5.16 distance with C-24, C-26 and C-27; LEU-1675 at 3.89, 4.80 and 2×4.96 with C-26 and C-27; LEU-1668 at 5.33 distance with C-28; TRP-1490 at 4.63, 5.41 distance with C-29; and LYS-1671 at 3.84, 4.30, 4.53 distance with C-28 and C-30.

Anticancer activities were done on human cancer cell lines MDA-MB-231, BT-549, A-549, and SW-480. Molecular interaction of these activities was successfully confirmed by inhibition of the PI3Kα/AKT/mTOR signaling pathway, *in silico*.

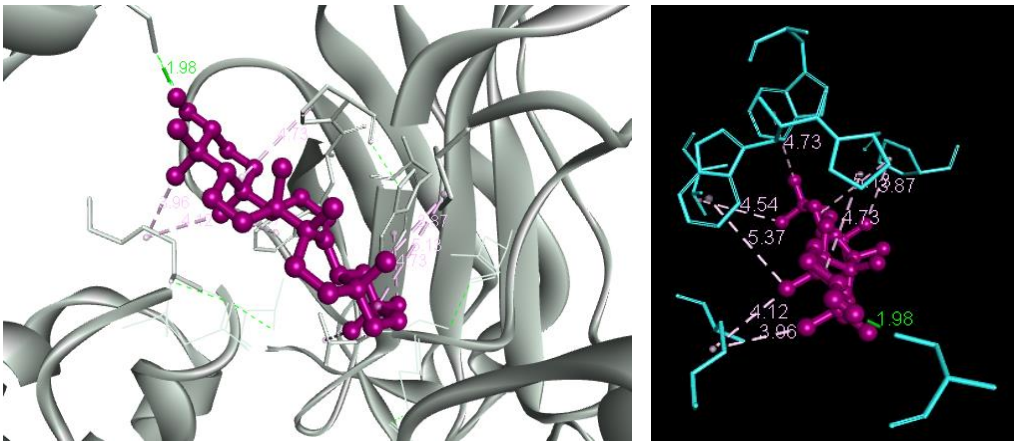

(A) **(B)**

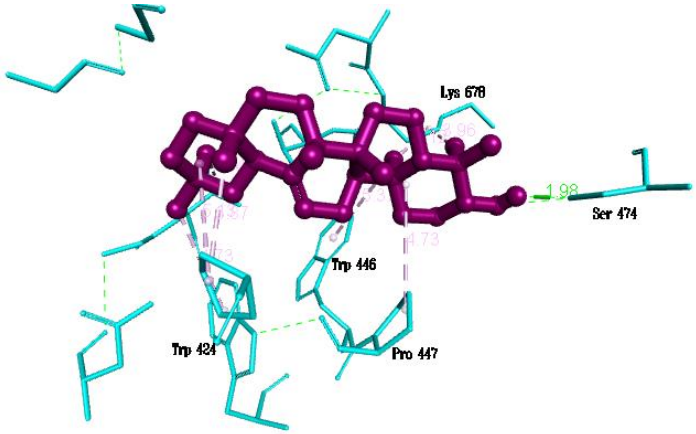

(C)

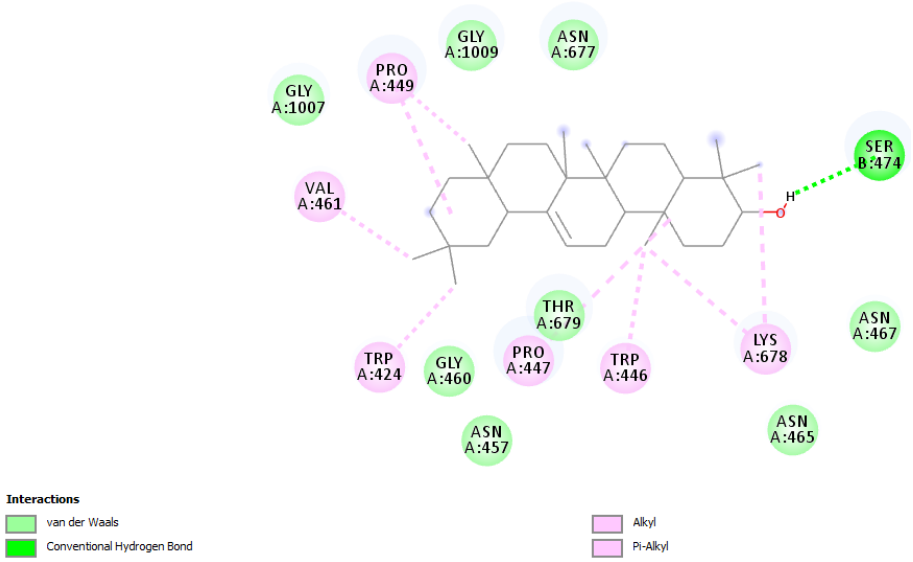

(D)

Ligand (*β*-amyrin)

Figure 3. (A) *β*-Amyrin (ball and stick) showing interaction with the active site of PI3K*α* (PDB: 4L23), (B) distance of ligand interaction with 4L23, and (C,D) hydrogen binding and hydrophobic interaction with amino acids

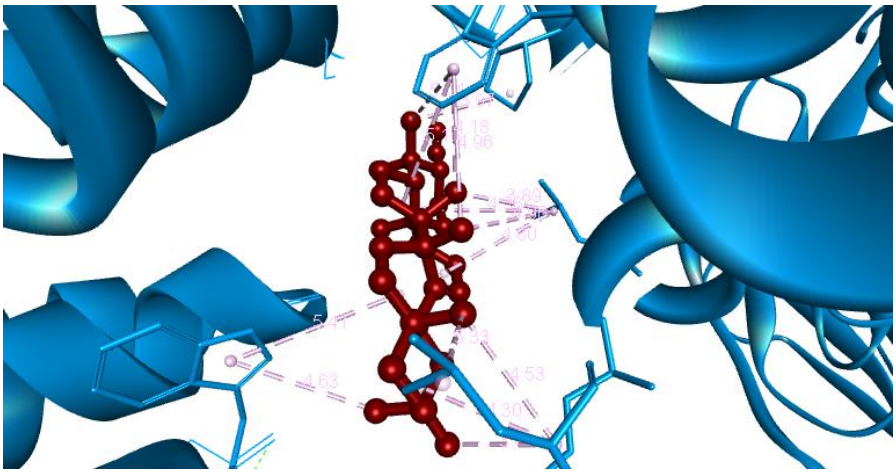

(A)

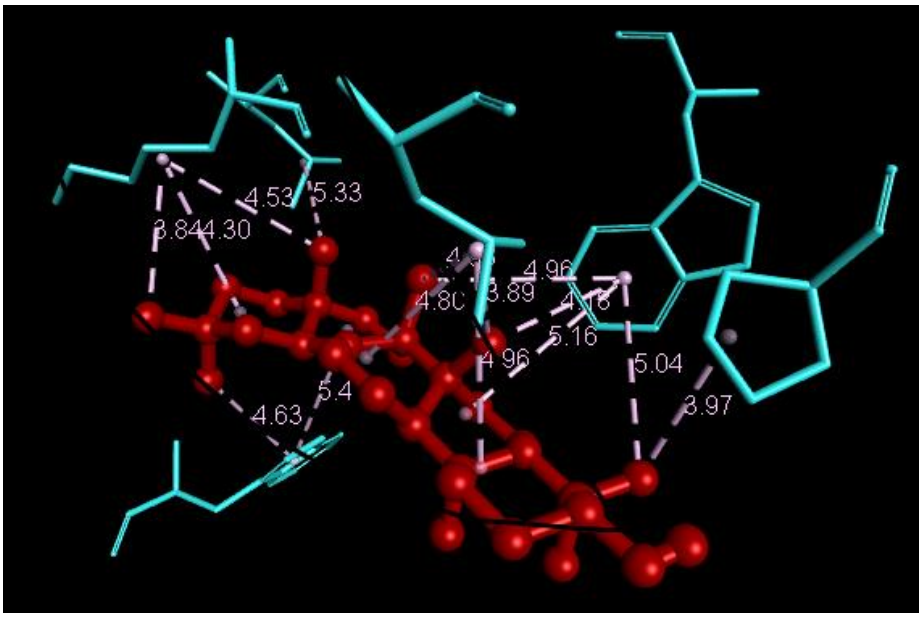
4.53
5.33
3.84
4.30
4.80
3.89
4.96
5.16
4.96
5.04
3.97
5.4
4.63

(B)

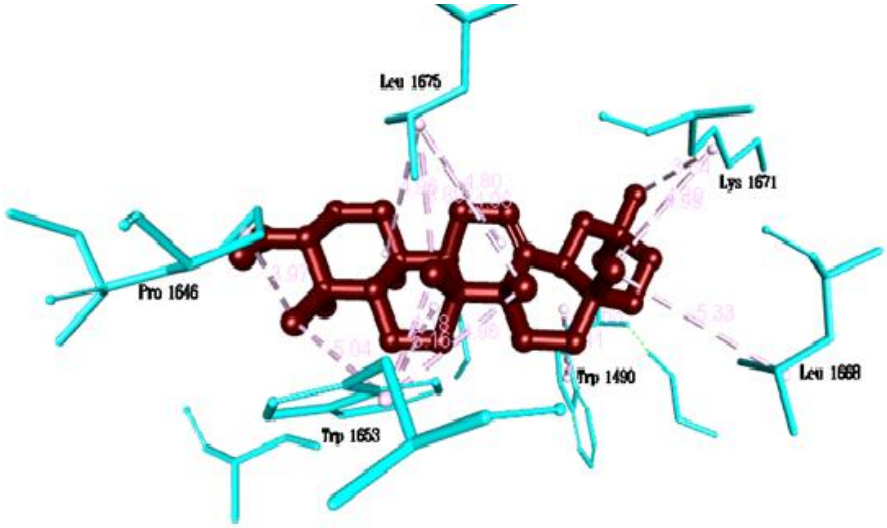
Leu 1675
Lys 1671
Pro 1646
Trp 1490
Leu 1668
Trp 1653

(C)

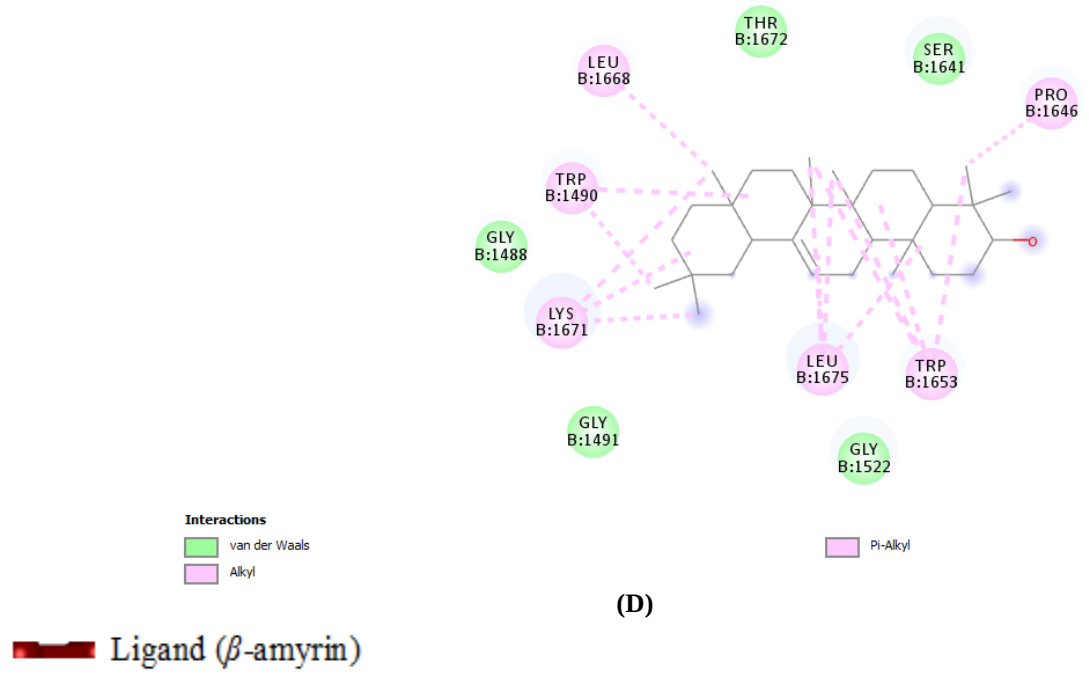

Figure 4. (A) Binding interaction of *β*-amyrin with the active site of mTOR (PDB: 4JT6), (B) distance of interaction between ligand and 4JT6, and (C, D) hydrophobic interaction of ligand with 4JT6

DISCUSSION

Bombax ceiba has high importance in herbal medicine and the main constituents are flavonoids, terpenoids, fatty acid, and steroids. Diethyl ether and light petroleum extracts of this plant have been used against A375, ACHN, LNCaP, HeLa, MCF-7, COR-L23, and C-32 human cancer cell lines [53]. *β*-amyrin has been used for anti-cancer activities on HEK-293, HepG2, Caco-2, [54] and HK-1 [55] human cancer cell lines. Our studies have focused on the anticancer activities of the leaf extract and *β*-amyrin on MDA-MB-231, SW480, A549, and BT549 cancer cells lines (*in vitro*). From Figure 2A, we found the EtOH leaf extract at the concentration of 100 µg/ml showed the best inhibitory effect on breast cancer cell line BT-549 (54% cell viability), and from Figure 2B, *β*-amyrin at the concentration of 100 µg/ml exhibited high inhibitory effect on breast cancer cell lines MDA-MB-231 (58% cell viability) and BT-549 (57% cell viability). BT-549 is a human breast cancer cell line which showed better inhibitory concentration than SW-480, A-549, and MDA-MB-231 cancer cell lines. When we compare Figure 2A (leaf extract) and Figure 2B (*β*-amyrin), we find that the leaf extract showed more inhibitory effect on the four cancer cell lines.

β-amyrin was further investigated on various proteins such as EGFR, AKT, P^{53}, IGFR, KRAS, PI3K, mTOR, BCl2, PDK, Tankyrase, PTEN, etc., *in silico*, for best inhibition of signaling pathways. Best investigation results were shown by mTOR (Table 2, entry 8), PI3Kβ (Table 2, entry 12), and P^{53} (Table 2, entry 1). PI3Ks are subdivided into four catalytic subunits, PI3Kα, PI3Kβ, PI3Kγ, and PI3Kδ. So, PI3K was further investigated at the subunit level and we found the best result by PI3Kα (Table 2, entry 11). Finally, we found that PI3Kα has a high binding energy, with mTOR being very close. So, *β*-amyrin may be useful in inhibition of PI3K and mTOR kinases.

PI3Ks are lipid kinases involved in the regulation of various cellular processes including proliferation, survival, migration, metabolism, metastasis, etc. [56-57]. The PI3K family of signal-transducing enzymes are divided into three classes (I, II, and III). Class I is responsible for catalyzing PIP_2 (phosphorylation of phosphatidylinositol 4,5 diphosphate) to PIP_3 (phosphatidylinositol 3,4,5-triphosphate) [58]; PIP_3 is regulated by PTEN (phosphatase and tensin homologue protein) [59]. A second messenger PIP_3 is responsible for activation of serine-threonine kinase AKT, which plays a key role in promotion of cellular processes, including survival, cell growth, proliferation, and metabolism [60-61]. Phosphorylation of AKT activates the mammalian target of rapamycin (mTOR), which plays an important role in promoting cell growth, proliferation, and survival by integrating signals from growth factors, cellular energy levels, and nutrient metabolism [62].

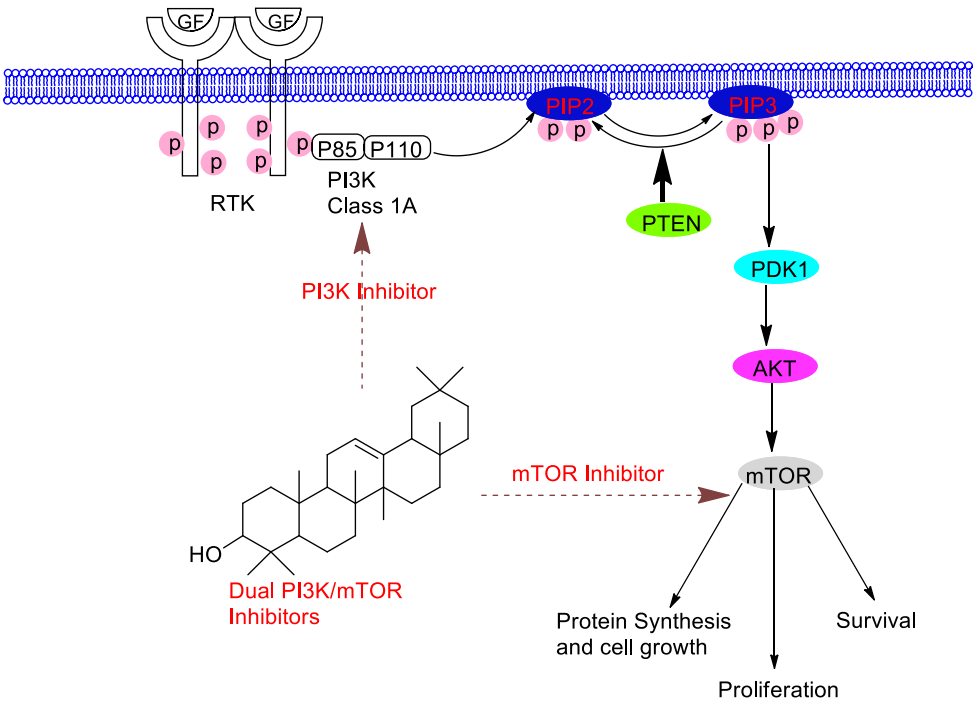

Figure 5. Overview of PI3K/AKT/mTOR signaling pathway. Active compound targets PI3Kα and mTOR.

In cancer, class IA PI3K and PI3Kα isoform are promising therapeutic targets on the identification of activating mutations in PI3Kα subunit and loss of function of phosphatase and tensin homolog protein (PTEN) in a notable percentage of solid human tumors, such as breast, ovarian, prostate, and colon cancers [63]. The target of the PI3K pathway is an important emerging approach for the treatment of cancers because a high percentage of human cancers are revealed to rely strongly on PI3K*α* for resistance and survival to various targeted cancer therapies [64-65]. It has been revealed from the literature that various external factors such as nutrient intake and growth factors can activate AKT and mTOR, and bypass PI3K, thus restarting cancer genesis [66-67]. For this reason, *β*-amyrin targets of both PI3K and mTOR may more effectively prevent tumors with multiple pathway activations. Dual kinase inhibitor PI3K/mTOR represents a beneficial therapeutic intervention strategy in the treatment of cancer therapies. *β*-amyrin targets of PI3Kα and mTOR are summarized in Figure 5.

CONCLUSION

In summary, *β*-amyrin was isolated from the leaf extract of *Bombax ceiba* plant and the structure was elucidated by spectroscopic methods, which included 1D-NMR, 2D-NMR, and HR-MS. The anticancer activity was evaluated on breast, colon, and lung cancer cell lines. The best results were displayed on breast cancer cell lines BT-549 by the leaf extract and MDA-MB-231 by β-amyrin at 100 µg/ml. The docking studies displayed best docking score results with PI3Kα and mTOR, which indicates that the isolated compound has higher probability of targetting the PI3K/AKT/mTOR signaling pathway. Thus, the compound and extract are both beneficial in cancer therapy treatments.

Conflicts of Interest

The authors do not have any conflicts of interest.

ACKNOWLEDGMENTS

The authors would like to thank the Chairman, Department of Chemistry, A.M.U, Aligarh for providing necessary lab facilities. The authors also thank SAIF, PU, Chandigarh for providing the spectroscopic data. The leaves of *Bombax ceiba* plant were collected from the area in Bisalpur, Pilibhit District, UP, India-262201 and authenticated by Taxonomy and Ethnobotany professor M. Badruzzaman Siddiqui, AMU, Aligarh-202002 India (Accession No. 31979).

REFERENCES

1. Maiden, J. H. (1889) The useful native plants of Australia: Including Tasmania, Turner and Henderson, Sydney.

2. Agnivesha-Charak-Dridhabala (2000) Charak Samhita Sutrasthana, chapter 4, Shloka 5, 31, 75, 46 and 77, 2nd edition, Chaukhamba Sanskrit Pratishthan, Delhi.

3. Gyatso, T. and Hakim, C. (2010) Essentials of Tibetan traditional medicine, North Atlantic books, California.

4. Kabir, H. (2002) Introduction to Ilmul Advia, Shamsher Publishers and Distributors, Aligarh.

5. Liu, Z. (2009) Essentials of Chinese medicine, Springer, Germany.

6. Vagbhatta (1993) Ashtang Hridya Sutrasthana chapter 15, Shloka 37-39, 11 edition, Chawkhamba Sanskrit Sansthan, Varanasi.

7. Mitra, S. and Mukharjee, S. (2009) Some Abortifacient plants used by the tribal people of West Bengal, *Nat Prod Radia*, **8(2)**, 167–171.

8. Ghose, T. P. (1935) Bombax malabaricum, *Indian Forester*, **61**, 93–103.

9. Refaat, J., Desoky, S. Y. and Ramadan, M. A. (2013) Bombacaceae A phytochemical review, *Pharm Biol.*, **51**, 100–130.

10. Faizi, S. and Ali, M. (1999) Shamimin A new flavonol C glycoside from leaves of Bombax ceiba, *Planta Med.*, **65**, 383-385.

11. Singh, G., Passsari, A. K. and Leo, V. V. (2016) Evaluation of phenolic content variability along with antioxidant, antimicrobial, and cytotoxic potential of selected traditional medicinal plants from India, *Front Plant Sci.*, **7**, 407.

12. Tundis, R., Rashed, K. and Said, A. (2014) In vitro cancer cell growth inhibition and antioxidant activity of *Bombax ceiba* (Bombacaceae) flower extracts, *Nat. Prod. Commun.*, **9**, 691.

13. Mostafa, N. M. (2018) β-Amyrin Rich Bombax ceiba Leaf Extract with Potential Neuroprotective Activity against Scopolamine-Induced Memory Impairment in Rats, *Rec. Nat. Prod.*, **12(5)**, 480–492.

14. de-Almeida, S. C. X., da-Silva, A. C. F. and Sousa, N. R. T. (2019) Antinociceptive and anti-inflammatory activities of a triterpene-rich fraction from Himatanthus drasticus, *Braz. J. Med. Biol Res.*, **52(5)**, 7798.

15. de Almeida, P. D. O., de A. Boleti, A. P. and Rüdiger, A. L. (2015) Anti-inflammatory activity of triterpenes isolated from *protium paniculatum* oil-resins, *Evid Based Complement Alternat Med.*, **10,** 293768.

16. Cardoso, B. K., Marko de Oliveira, H. L. and Melo, U. Z. (2020) Antioxidant activity of α and β-amyrin isolated from Myrcianthes pungens leaves, *Nat. Prod. Res.*, **34(12)**, 1777–1781.

17. Pinto, S. A. H., Pinto, L. M. and Cunha, G. M. (2008) Anti-inflammatory effect of alpha, beta-Amyrin, a pentacyclic triterpene from Protium heptaphyllum in rat model of acute periodontitis, *Inflammo pharmacol*, **16(1)**, 48–52.

18. Melo, C. M., Morais, T. C. and Tome, A. R. (2011) Anti-inflammatory effect of alpha,beta-amyrin, a triterpene from Protium heptaphyllum, on cerulein-induced acute pancreatitis in mice, *Inflamm Res.*, **60**, 673–681.

19. Nair, S. A., Sabulal, B. and Radhika, J. (2014) Promising anti-diabetes mellitus activity in rats of beta-amyrin palmitate isolated from Hemidesmus indicus roots, *Eur. J. Pharmacol.*, **734**, 77–82.

20. Santos, F. A., Frota, J. T. and Arruda, B. R. (2012) Antihyperglycemic and hypolipidemic effects of alpha, beta-amyrin, a triterpenoid mixture from Protium heptaphyllum in mice, *Lipids Health Dis.*, **11**, 98.

21. Maiyo, F., Moodley, R. and Singh, M. (2016) phytochemistry, cytotoxicity and apoptosis studies of β-sitosterol-3-o-glucoside and β -amyrin from prunus africana, *Afr J Tradit Complement Altern. Med.*, **13(4)**, 105–112.

22. Park, H. J., Kwon, H. and Lee, J. H. (2020) β-Amyrin Ameliorates Alzheimer's Disease-Like Aberrant Synaptic Plasticity in the Mouse Hippocampus, *Biomol Ther (Seoul)*, **28(1)**, 74–82.

23. Santos, F. A., Frota, J. T. and Arruda, B. R. (2012) Antihyperglycemic and hypolipidemic effects of α, β-amyrin, a triterpenoid mixture from Protium heptaphyllum in mice, *Lipids Health and Dis*, **11**, 98.

24. Srikanth, M., Rao, B. G. and Rao, T. M. (2013) Anticancer activity of various extracts of Musa rosacea, Avicennia marina and Bombex ceiba, *Int. J. Pharm. Pharm. Sci.*, **5(4)**, 553–555.

25. Ullah Jan, H. T., Ali, S. M., Shabbir, A., Nasir, B. and Zahra, S. S. (2017) Revealing the cytotoxic potential of medicinal folklore: Bombax ceiba L, *J. Biores. Manag.*, **4(3)**.

26. Wen, S., Gu, D. and Zeng, H. (2018) Antitumor effects of beta-amyrin in Hep-G2 liver carcinoma cells are mediated via apoptosis induction, cell

cycle disruption and activation of JNK and P38 signalling pathways, *J. BUON*, **23(4)**, 965–970.

27. Maiyo, F., Moodley, R. and Singh, M. (2016) Phytochemistry, cytotoxicity and apoptosis studies of β-sitosterol-3-*o*-glucoside and β -amyrin from prunus africana, *Afr. J. Tradit. Complement Altern. Med.*, **13(4)**, 105–112.

28. Mishra, T., Arya, R. K., Meena, S., Joshi, P., Pal, M., Meena, B., Upreti, D. K., Rana, T. S. and Datta, D. (2016) Isolation, characterization and anticancer potential of cytotoxic triterpenes from Betula utilis bark, *PLoS ONE*, **11(7)**, 0159430.

29. Li, Z., Ge, H. Z., Xie, Y. G. and Shi, L. (2016) Design and synthesis of triazolyl-napthyl derivative of β-amyrin and its *in vitro* anti-cancer and apoptotic activities in human nasopharyngeal carcinoma (HK-1) cell line, *Bangladesh J. Pharmacol.*, **11**, 168–174.

30. Engelman, J. A. (2009) Targeting PI3K signalling in cancer: opportunities, challenges and limitations, *Nat. Rev. Cancer*, **9(8)**, 550–562.

31. Hanahan, D. and Weinberg, R. A. (2011) Hallmarks of cancer: the next generation, *Cell*, **144(5)**, 646–674.

32. Lien, E. C., Dibble, C. C. and Toker, A. (2017) PI3K signaling in cancer: beyond AKT, *Curr. Opin. Cell Biol.*, **45**, 62–71.

33. Martini, M., De Santis, M. C., Braccini, L., Gulluni, F. and Hirsch, E. (2014) PI3K/AKT signaling pathway and cancer: an updated review, *Ann. Med.*, **46(6)**, 372–383.

34. Fruman, D. A. and Rommel, C. (2014) PI3K and cancer: lessons, challenges and opportunities, *Nat. Rev. Drug Discov.*, **13(2)**, 140–156.

35. Davis, N. M., Sokolosky, M. and Stadelman, K. (2014) Deregulation of the EGFR/PI3K/PTEN/ Akt/mTORC1 pathway in breast cancer: possibilities for therapeutic intervention, *Oncotarget*, **5(13)**, 4603–4650.

36. Bendale, Y., Bendale, V., Paul, S. (2017) Evaluation of cytotoxic activity of platinum nanoparticles against normal and cancer cells and its anticancer potential through induction of apoptosis, *Integr. Med. Res.*, **6(2)**, 141–148.

37. Henneh, I. T., Huang, B., Musayev, F. N., Hashimi, R. A., Safo, M. K., Armah, F. A., Ameyaw, E. O., Adokoh, C. K., Ekor, M. and Zhang, Y. (2020) Structural elucidation and in vivo anti-arthritic activity of β-amyrin and polpunonic acid isolated from the root bark of Ziziphus abyssinica HochstEx. A Rich (Rhamnaceae), *Bioorg. Chem.*, **98**, 103744.

38. Okoye, N. N., Ajaghaku, D. L., Okeke, H. N., Ilodigwe, E. E., Nworu, C. S. and Okoye, F. B. C. (2014) Beta-Amyrin and alpha-amyrin acetate isolated from the stem bark of Alstonia boonei display profound anti-inflammatory activity, *Pharm. Biol.*, **52(11)**, 1478–1486.

39. Mejin, M. (2009) Isolation, structural elucidation and antibacterial activity of the chemical constituents of Scaevola spinescens, Ph.D. Thesis, The University of Adelaide, Australia.

40. Amiri, M. T., Bertella, S., Questell-Santiago, Y. M. and Luterbacher, J. S. (2019) Establishing lignin structure-upgradeability relationships using quantitative 1H–13C heteronuclear single quantum coherence nuclear magnetic resonance (HSQC-NMR) spectroscopy, *Chem. Sci.*, **10**, 8135.

41. Lee, J. J. X., Loh, K. and Yap, Y. S. (2015) PI3K/Akt/mTOR inhibitors in breast cancer, *Cancer Biol. Med.*, **12**, 342-354.

42. Lin, H. J., Hsieh, F. C. and Song, H. (2005) Elevated phosphorylation and activation of PDK-1/AKT pathway in human breast cancer, *Br. J. Cancer*, **93**, 1372 – 1381.

43. Nassiri, I., Faghihi, M. and Tavassoli, M. (2009) Pharmacogenomic Profiling of the PI3K/PTEN Pathway in Sporadic Breast Cancer, *Iranian Biomed. J.*, **13(2)**, 79–86.

44. Davis, N. M., Sokolosky, M. and Stadelman, K. (2014) Deregulation of the EGFR/PI3K/PTEN/ Akt/mTORC1 pathway in breast cancer: possibilities for therapeutic intervention, *Oncotarget*, **5(13)**, 4603-4650.

45. Drury, S. C., Detre, S. and Leary, A. (2011) Changes in breast cancer biomarkers in the IGF1R/PI3K pathway in recurrent breast cancer after tamoxifen treatment, *Endocr Relat Cancer*, **18(5)**, 565–577.

46. Navolanic, P. M., Steelman, L. S. and McMahon, M. (2004) Activation of the PI3K/PDK/Akt signal transduction pathway decreases *in vitro* sensitivity of MCF-7 breast cancer cells to doxorubicin and 4-hydro-xytamoxifen, *Proc. Amer. Assoc. Cancer Res.*, **45**.

47. Girnius, N., Edwards, Y. J. K. and Garlick, D. S. (2018) The cJUN NH_2-terminal kinase (JNK) signaling pathway promotes genome stability and prevents tumor initiation, *eLife*, **7**, 36389.

48. Ahmad, D. A. J., Negm, O. H. and Alabdullah, M. L. (2016) Clinicopathological and prognostic significance of mitogenactivated protein kinases (MAPK) in breast cancers, *Breast Cancer Res. Treat*, **159**, 457–467.

49. Khan, N., Afaq, F., Khusro, F. H., Adhami, V. M., Suh, Y., Mukhtar, H. (2012) Dual inhibition of phosphatidylinositol 3-kinase/Akt and mammalian target of rapamycin signaling in human nonsmall cell lung cancer cells by a dietary flavonoid fisetin, *Int. J. Cancer*, **130**, 1695–1705.

50. Tewari, D., Patni, P., Bishayee, A., Sah, A. N., Bishayee, A. (2019) Natural products targeting the PI3K-Akt-mTOR signaling pathway in cancer: A novel therapeutic strategy, *Semin. Cancer Biol.*, **S1044-579X(19)**.

51. Huang, S. (2013) Inhibition of PI3K/Akt/mTOR Signaling by Natural Products, *Anticancer Agents Med. Chem.*, **13(7)**, 967–970.

52. Sun, H., Wang, Z., Yakisich, J. S. (2013) Natural products targeting autophagy via the PI3K/ Akt/mTOR pathway as anticancer agents, *Anticancer Agents Med Chem*, **13(7)**, 1048–1056.

53. Tundisa, R., Rashedb, K., Saidb, A., Menichinia, F. and Loizzoa, M. R. (2014) In vitro cancer cell growth inhibition and antioxidant activity of bombax ceiba (bombacaceae) flower extracts, *Nat. Prod. Commun.*, **9(5)**, 691–694.

54. Maiyo, F., Moodley, R. and Singh, M. (2016) Phytochemistry, cytotoxicity and apoptosis studies of β-sitosterol-3-*o*-glucoside and β -amyrin from prunus africana, *Afr. J. Tradit. Complement Altern. Med.*, **13(4)**, 105–112.

55. Li, Z., Ge, H. Z., Xie, Y. G. and Li, S. (2016) Design and synthesis of triazolyl-napthyl derivative of β-amyrin and its in vitro anti-cancer and apoptotic activities in human nasopharyngeal carcinoma (HK-1) cell line, *Bangladesh J. Pharmacol*, **11**, 168–174.

56. Wymann, M. P. and Schneiter, R. (2008) Lipid signalling in disease, *Nat. Rev. Mol. Cell Biol.*, **9**, 162–176.

57. Engelman, J. A. (2009) Targeting PI3K signalling in cancer: opportunities, challenges and limitations, *Nat. Rev. Cancer*, **9**, 550–562.

58. (a) Cantley, L. C. (2002) The phosphoinositide 3-kinase pathway, *Science*, **296**, 1655–1657.

    (b) Engelman, J. A., Luo, J. and Cantley, L. C. (2006) The evolution of phosphatidylinositol 3-kinases as regulators of growth and metabolism, *Nat. Rev. Genet.*, **7**, 606–619.

59. Carracedo, A. and Pandolfi, P. P. (2008) The PTEN-PI3K pathway: of feedbacks and cross talks, *Oncogene*, **27**, 5527–5541.

60. Bader, A. G., Kang, S. and L. Zhao. (2005) Oncogenic PI3K Deregulates Transcription and Translation, *Nat. Rev. Cancer*, **5**, 921–929.

61. Manning, B. D. and Cantley, L. C. (2007) AKT/PKB Signaling: Navigating Downstream, *Cell*, **129**, 1261–1274.

62. Guertin, D. A. and Sabatini, D. M. (2007) Defining the role of mTOR in cancer, *Cancer Cell*, **12**, 9–22.

63. (a) Shayesteh, L., Lu, Y. and Kuo, W. L. (1999) PIK3CA is implicated as an oncogene in ovarian cancer, *Nat. Genet.*, **21**, 99–102.

    (b) Samuels, Y., Wang, Z. and Bardelli, A. (2004) High frequency of mutations of the PIK3CA gene in human cancers, *Science*, **304**, 554.

    (c) Parsons, D. W., Wang, T. L. and Samuels, Y. (2005) Colorectal cancer: mutations in a signalling pathway, *Nature*, **436**, 792.

64. Liu, P., Cheng, H. and Roberts, T. M. (2009) Targeting the phosphoinositide 3-kinase pathway in cancer, *Nat. Rev. Drug Discovery*, **8**, 627–644.

65. Hollander, M. C., Blumenthal, G. M. and Dennis, P. A. (2011) PTEN loss in the continuum of common cancers, rare syndromes and mouse models, *Nat. Rev. Cancer*, **11**, 289–301.

66. Peng, T., Golub, T. R. and Sabatini, D. M. (2002) The immunosuppressant rapamycin mimics a starvation-like signal distinct from amino acid and glucose deprivation, *Mol. Cell Biol.*, **22**, 5575–5584.

67. Shaw, R. J. and Cantley, L. C. (2006) Ras, PI3K and mTOR signaling controls tumour cell growth, *Nature*, **441**, 424–430.

Graphical abstract:

β-amyrin is a biologically active compound that was isolated from EtOH extract of *B. ceiba* leaves. This figure shows the anticancer activity of the leaves extract and isolated compound against human breast (MDA-MB-231 and BT-549), lung (A-549) and colon (SW-480) cancer cell lines. The docking studies of the isolated compound was exhibited a best docking score with PI3K and mTOR kinases.